Biochemical and Biophysical Research Communications 463 (2015) 123–129

Contents lists available at ScienceDirect

Biochemical and Biophysical Research Communications

journal homepage: www.elsevier.com/locate/ybbrc

Stable knockdown of Kif5b in MDCK cells leads to epithelial–mesenchymal transition

Ju Cui [a, b, *], Guoxiang Jin [b], Bin Yu [b], Zai Wang [b, c], Raozhou Lin [b], Jian-Dong Huang [b, d, *]

[a] The Key Laboratory of Geriatrics, Beijing Hospital & Beijing Institute of Geriatrics, Ministry of Health, Beijing, China
[b] Department of Biochemistry, LKS Faculty of Medicine, The University of Hong Kong, Hong Kong SAR, China
[c] Institute of Clinical Medical Sciences, China-Japan Friendship Hospital, Beijing, China
[d] The Centre for Synthetic Biology Engineering Research, Shenzhen Institutes of Advanced Technology, Shenzhen, China

ARTICLE INFO

Article history:
Received 28 April 2015
Available online 20 May 2015

Keywords:
Kif5b
MDCK cell
Epithelial–mesenchymal transtion

ABSTRACT

Polarization of epithelial cells requires vectorial sorting and transport of polarity proteins to apical or basolateral domains. Kif5b is the mouse homologue of the human ubiquitous Kinesin Heavy Chain (uKHC). To investigate the function of Kif5b in epithelial cells, we examined the phenotypes of Kif5b-deficient MDCK cells. Stable knockdown of Kif5b in MDCK cells resulted in reduced cell proliferation rate, profound changes in cell morphology, loss of epithelial cell marker, and gain of mesenchymal marker, as well as increased cell migration, invasion, and tumorigenesis abilities. E-cadherin and NMMIIA could interact with Kif5b in polarized MDCK cells, and their expression levels were decreased in Kif5b-deficient MDCK cells. Overexpression of E-cadherin and NMMIIA in Kif5b depleted MDCK cells could decrease mesenchymal marker expression and cell migration ability. These results indicate that stable knockdown of Kif5b in MDCK cells can lead to epithelial–mesenchymal transition, which is mediated by defective E-cadherin and NMMIIA expression.

1. Introduction

The polarity is a fundamental feature of many eukaryotic cells. In a study of *Caenorhabditis elegans* development, it was found that centrosomes or associated microtubules provide an essential cue for the specification of the body polarity axis [1]. Microtubules act as structural components and participate in the regulation of many cellular activities, including cell division and intracellular transportation [2]. Therefore, microtubules and their associated motor proteins (kinesin and dynein) are indispensable for delivering proteins related to polarity establishment and maintenance. Using polarized transport assay in permeabilized MDCK cells, Lafont et al. [3] found that both apical and basolateral transport require microtubule motors and that cytosolic kinesin is responsible for basolateral transport, while both dynein and kinesin are involved in apical transport.

Several kinesin family proteins have been reported to be involved in apical transport in epithelial cells. KIF3A has been shown to mediate the interaction of the polarity protein Par3/Par6/aPKC complex with microtubules in polarized MDCK cells [4]. KIFC3, a minus end-directed microtubule motor protein, is identified and characterized for apical transport of annexin XIIIb-associated vesicles [5]. Post-Golgi transport of p75 to apical membrane in polarized MDCK cells is mediated by Kif5b (the heavy chain of Kinesin-1) [6]. Kinesin-1 also participates in the basolateral trafficking of Na^+-K^+ ATPase in alveolar epithelial cells [7]. Furthermore, p120 catenin forms a complex with Kif5b to facilitate the transport of N-cadherin-catenin complexes to adhesion junctions in HeLa cells [8], indicating that Kif5b might be involved in E-cadherin transport in epithelial cells. Moreover, in colonic epithelial cells, Kif5b is localized at intact and internalized apical junctions and can mediate the disassembly and internalization of adhesion junctions and tight junctions upon Ca^{2+} depletion [9]. In the adult mouse kidney, Kif5b is selectively and asymmetrically expressed in the basolateral domain of epithelial cells in the thick ascending limbs and distal convoluted tubules, and knockout of Kif5b leads to depolarization of Na^+-K^+ ATPase [10].

Against this background, and as a first step in obtaining clues to the functions of Kif5b in epithelial cells, we have employed RNAi technology to knockdown of Kif5b in MDCK cells and examined the phenotypes of Kif5b-deficient cells.

* Corresponding authors. The Key Laboratory of Geriatrics, Beijing Hospital & Beijing Institute of Geriatrics, Ministry of Health, Beijing, China. Fax: +86 10 65132982.
E-mail addresses: juzi.cui@gmail.com (J. Cui), jdhuang@hku.hk (J.-D. Huang).

http://dx.doi.org/10.1016/j.bbrc.2015.05.045
0006-291X/

2. Materials and methods

2.1. DNA constructs

The Kif5b-shRNA expression plasmid was constructed based on the p*Silencer* 3.1-H1 hygro siRNA expression system (Roche). Two siRNA sequences were selected (target 1: 5′-GCCTTATGCATTT-GACCGA-3'; target 2: 5′-ACACCTCTCAAGAGCAAGT-3′). Mouse Cdh1 and Myh9 cDNA was amplified by RT-PCR from mouse kidney and subcloned into pcDNA3.1.

2.2. Cell culture

Canine MDCK cells were obtained from the HKU-Pasteur Research Centre, HKU and were cultured in DMEM (Invitrogen) supplemented with 10% FBS (Gibco) in a humidified atmosphere with 5% CO_2 at 37 °C. The p*Silencer*^{TM} 3.1-H1 hygro Kif5b-siRNA plasmids were transfected into the MDCK cells using FuGENE 6 transfection reagent (Roche), and 350 μg/ml hygromycin (Roche) was used to select stable cells. PolyJet (SignaGen) was used for transient transfection of plasmid DNA into the Kif5b deficient MDCK cells.

2.3. Cell proliferation assays

1×10^3 cells were seeded into 96-well plate and incubated overnight. At different time points, the culture medium was replaced with medium containing 20 μl of MTT dye (5 mg/ml, Sigma). After incubation at 37 °C for 3.5 h, the medium was carefully removed, and 150 μl DMSO was added to dissolve the formazan crystals. The absorbance was read at 570 nm using a SpectraMAX 340 microplate spectrophotometer. For live cell counting, 1×10^4 cells were seeded into a 6-well plate. After incubation for one day, cells were trypsinized and stained by trypan blue. The live cells were visualized and counted under an inverted microscope (Nikon). All experiments were repeated five times.

2.4. Cell-cycle analysis

Cells were trypsinized at 48 h after being seeded into 3.5 cm dishes. The harvested cells were fixed with 4% paraformaldehyde for 30 min and permeabilized with 70% ethanol for at least 1 h. After washing in PBS, 200 μg/ml RNase was added to the cell suspensions and allowed to react for 30 min at room temperature. Propidium iodide (25 μg/ml) was added to stain the cells for 10 min on ice. After washing in PBS, the cells were subjected to flow cytometry (Beckman Coulter) using a 488 nm argon-ion laser. A single cell population was ensured using FS/SS gating during analysis. The cell-cycle analysis was performed using ModFit LT 2.0 software.

2.5. In-vitro cell migration assay

Cells were seeded at a density of 3×10^5 cells per well in a 6-well plate. A wound was incised 24 h later in the central area of the confluent culture. The cells were then carefully washed with PBS to remove the detached cells, and cultured for another 24 h in fresh medium. Photos were taken under inverted microscopy.

2.6. Tumorigenicity assay in nude mice

Mouse experimentation was carried out in strict accordance with the recommendations in the guide for the Care and Use of Laboratory Animals of the United States National Institutes of Health. The protocol was approved by the Committee on the Use of Live Animals in Teaching and Research at the University of Hong Kong (Permit Number: 2375-11). 1×10^6 cells suspended in 0.1 ml of PBS were subcutaneously injected into nude mice at the neck and flanks. The animals were examined for tumor formation over a period of 1.5 months.

2.7. Western blot

Cells were washed with PBS and lysed in buffer (10 mM Tris-Cl (pH 7.4), 0.15 M NaCl, 5 mM EDTA, 1% Triton X-100). Protein levels were determined by blotting with anti-Kif5b primary antibody (1:2000, [11]), anti-Kinesin II (1:1000, Covance), anti-Kif4A (1:1000, Bethyl); anti-KLC (a gift from Dr ST Brady, University of Illinois at Chicago); anti-actin (1:3000, Sigma); anti-E-cadherin (1:2000, BD); anti-N-cadherin (1:2000, BD); anti-Vimentin (1:1000, Santa Cruz); anti-β-catenin (1:1000, BD); and anti-NMMIIA (1:1000, Covance). An enhanced chemiluminescence kit (Pierce) was used to detect of the immune-reactive bands.

2.8. Co-immunoprecipitation

Polarized adherent MDCK cells were lysed in buffer containing 10 mM Tris-Cl (pH7.4), 0.15 M NaCl, 5 mM EDTA, 1% Triton X-100 and proteinase inhibitor. Cell debris was removed by centrifuging at 16,000 g at 4 °C for 15 min. The supernatant was incubated with protein A agrose beads pre-bound with antibodies for overnight at 4 °C. After washing in lysis buffer, beads were pelleted and suspended in SDS sample loading buffer. Proteins in supernatant were separated by 8% SDS-PAGE and analyzed by silver staining and western blot.

3. Results

3.1. Kif5b deficient cells exhibit a reduced proliferation rate

Fig. 1A is a representative Western blot of selected stable cell clones. Kif5b expression levels in control clones were comparable to those in wild-type MDCK cells, whereas Kif5b expression levels in cells transfected with Kif5b-shRNA varied. Kinesin II, Kif4A, Kif17, and KLC were expressed in wild-type MDCK cells, and Kif5b-targeting shRNA had no effect on the expression of these proteins.

It has been found that conditional knockout of Kif5b in mouse pancreatic β-cells [11] affect cell proliferation. MTT assays were carried out to evaluate whether the proliferation of Kif5b-deficient MDCK cells was affected. (Fig. 1B). Due to hygromycin selection, MDCK-CT cells had a lower proliferation rate than wild-type cells, and there was no difference among different MDCK-CT cell clones. However, knockdown of Kif5b significantly reduced cell proliferation rate in a Kif5b expression level dependent manner. The growth rates in cell clones SH-2, SH-7, and SH-9, in which Kif5b levels were reduced by about 50%, were lower than the growth rate in MDCK-CT cells, but higher than that of cell clones SH-6, SH-8, and SH-18, which had lower Kif5b expression levels. The decreased cell proliferation rate was further confirmed by counting viable cells stained with trypan blue (Fig. 1C).

FACS analysis demonstrated that Kif5b-deficient cells showed a higher proportion of cells in the G_0-G_1 phase, than did the control cells, and there were concomitant decreases in the proportion of cells in G_2/M phases. There was no significant difference in the proportion of S stage cells between control and Kif5b knockdown cells (Fig. 1C and Supplementary Fig. 1). These differences in cell-cycle distribution indicate that Kif5b is actively involved in regulation of the cell cycle in MDCK cells.

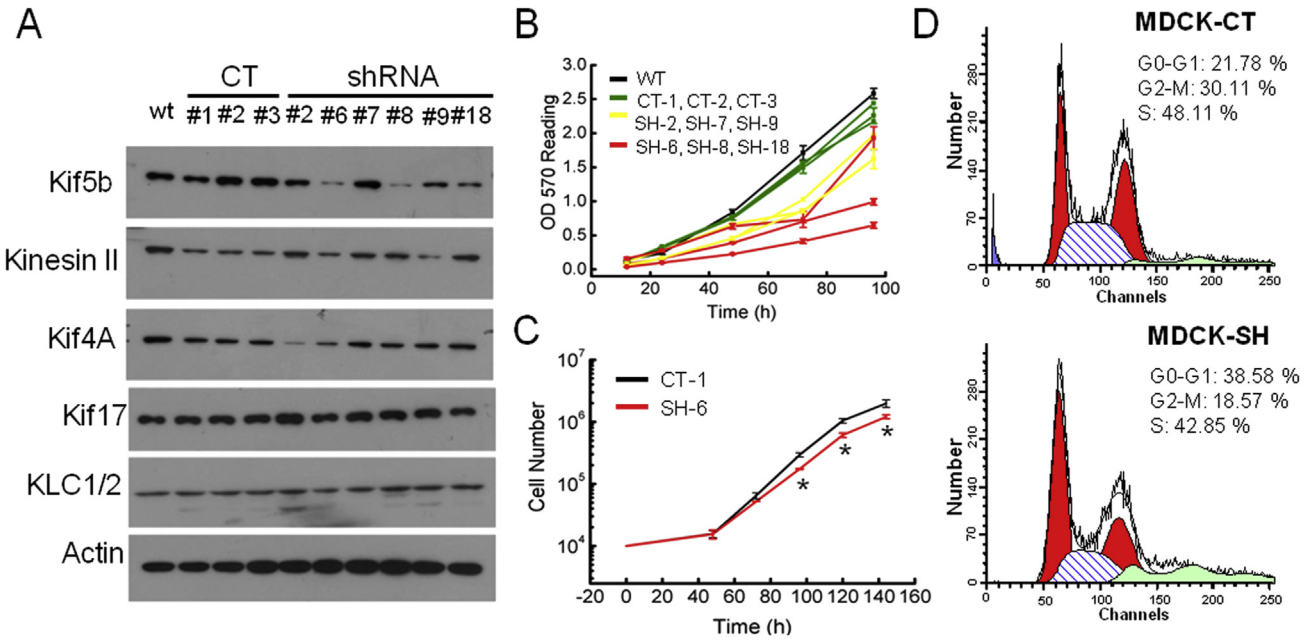

Fig. 1. shRNA-mediated knockdown of Kif5b in MDCK cells affects cell proliferation. (A) Representative Western blot results showed a reduction of Kif5b protein levels in *Kif5b*-shRNA transfected cells. Actin was used as an internal control. (B) Cell proliferation rates were analyzed by MTT assays. (C) Live cell numbers were counted at indicated time points (*$P < 0.05$). (D) A representative FACS analysis result. The percentages of cells in each cell-cycle phase are shown in each panel. Blue: apoptosis; red: G1 peak and G2 peak; shadow: S phase. (For interpretation of the references to colour in this figure legend, the reader is referred to the web version of this article.)

3.2. *Stable knockdown of Kif5b in MDCK cells induces an epithelial–mesenchymal transition*

In addition to a reduction in cell proliferation rate, it was also found that knockdown of Kif5b resulted in morphological changes of MDCK cells. The control cells displayed typical cobblestone-like cell shape as the wild-type cells. This morphological feature was observed in several independently isolated clones. By contrast, stable knockdown of Kif5b in MDCK cells made the cells detach from each other. These cells displayed a spindle-shaped morphology with extremely long membrane extensions. Moreover, many large and flattened cells with irregular shapes and two or more aggregated nuclei in the centre were found in Kif5b stable knockdown cells (arrows). These 'fused' cells consistently presented after several passages. Identical results were obtained in five independently isolated transfectant clones. To examine whether these large cells were senescent cells, the cells were stained using a senescence β-galactosidase staining kit (Cell Signaling). However, no positive blue staining could be detected in these cells, indicating that they do not result from senescence (data not shown).

To test whether stable knockdown of Kif5b in MDCK cells induces epithelial–mesenchymal transition, the expression levels of several epithelial–mesenchymal transition markers were examined by Western blot (Fig. 2B). It was found that a cadherin switch occurred due to knockdown of Kif5b. Control MDCK cells expressed a high level of E-cadherin, which is specifically expressed in epithelial cells. After knocking down of Kif5b, the E-cadherin level was substantially decreased, concomitant with higher expression of N-cadherin, indicating that Kif5b-deficient cells lost epithelial markers. Vimentin, a mesenchymal marker, was also analyzed in MDCK transfectants. Cells transfected by a control plasmid expressed low levels of Vimentin as previously reported in wild type MDCK cells [12], whereas Kif5b-deficient cells exhibited higher levels of this protein. The expression level of β-catenin was not significantly affected during this process.

The migratory properties of the transfectants were analyzed in a wound-healing assay (Fig. 2C). Kif5b-deficient cells exhibited a highly migratory ability and were able to migrate and completely heal the wound in the culture 24 h after the incision was made. By contrast, control cells moved toward the wound in a sheet and left the wound unhealed 24 h after the incision.

3.3. *Kif5b-depleted MDCK cells form larger metastatic tumors in nude mice*

Epithelial–mesenchymal transition has been implicated in the regulation of tumour development and metastasis [13]. To test the tumorigenic ability of Kif5b-deficient MDCK cells, both MDCK-CT and MDCK-SH cells were subcutaneously injected into athymic nu/nu mice at the neck and flanks. Kif5b-deficient MDCK cells exhibited stronger tumour formation ability in all injection sites on nude mice compared with control cells (arrows, Fig. 3A and Supplementary Fig. 2a). One month after injection, the tumor volume reached about 350 mm^3 in all five mice that received the injection of five different MDCK-SH cell clones. Tumor formation was also observed in mice injected with MDCK-CT cells, but the tumors were significantly smaller, ranging from 30 to 120 mm^3 (Fig. 3B).

In addition to having stronger tumorigenic ability, it was found that Kif5b knockdown cells exhibited a remarkable increase in metastatic foci on the lung (Fig. 3C), which was demonstrated by the appearance of white-yellow spots following picric acid staining. Histological analysis found that cells were well aligned, and could form tubules in tumours at the original inoculation sites (arrow heads) that were derived from MDCK-CT cells, suggesting that MDCK-CT cells retain proper polarity (Fig. 3D). Although many vacuoles (asterisks) were found in tumors developed from MDCK-SH cells, these vacuoles could not be considered tubular structures, because there were no tightly connected cells around each vacuole (Fig. 3D, left). In addition, kif5b knockdown cell showed increased migration and invasion abilities and could metastasize to

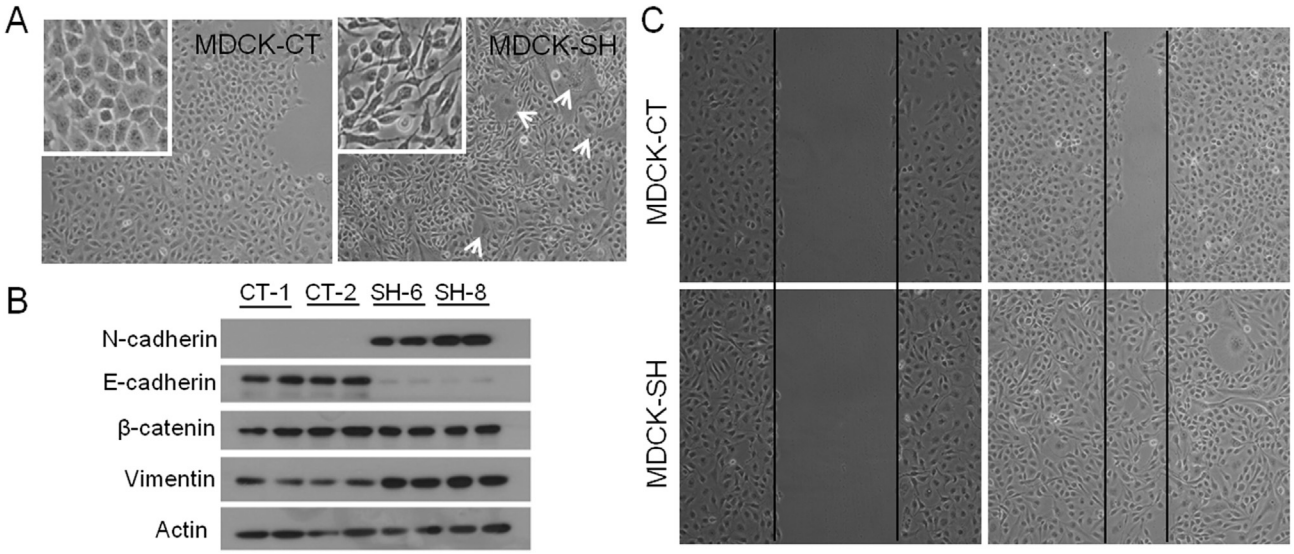

Fig. 2. Stable knockdown of Kif5b in MDCK cells induces an epithelial–mesenchymal transition. (A) A representative micrograph of both the control and the Kif5b knockdown cells at similar cell densities. Control cells, upper panel; MDCK-SH, lower panel. Many large and flattened cells with irregular shapes and two or more aggregated nuclei in the centre were found in MDCK-SH cells (arrows). (B) Western blot of the indicated proteins in control and Kif5b deficient MDCK cells. Samples were loaded in duplication. (C) The motility behavior of control (upper panel) and Kif5b deficient (lower panel) MDCK cells was analyzed in an *in vitro* wound-healing model. Photographs were taken immediately after incision (left panel) and after 24 h in culture (right panel). Identical results were obtained in five independently isolated transfectant clones.

lung whereas the control cell could not (Fig. 3D, right). Taken together, these results demonstrate that Kif5b-deficient MDCK cells loss cell polarity, gain migration and invasion abilities, and further indicate that these cells undergo epithelial–mesenchymal transition.

Owing to the mixture of cell types in tumors, it is unclear whether the larger tumors are actually derived from Kif5b-deficient cells. Because cells that were injected into nude mice carried the selection marker (hygromycin), they could be isolated by primary culture of tumor tissues. Tumor tissues were cut into small pieces with a volume of 1 mm^3, and then seeded into culture dishes. After two days, cells (designated P0) migrated out of the tissue cubes in both groups, but displayed distinct migration patterns (Fig. 3E). In tumors developed from MDCK-CT cells, the primary cells were found to migrate with a regular morphology, like cobblestones. However, the P0-SH cells that migrated out from tumors displayed irregular, elongated cell morphology, like fibroblasts.

The expression levels of several proteins were further examined for original stable cells (cell line), tumor tissues, and primary culture (Pri) cells (Fig. 3F). The reduction in Kif5b level was detected in both tumors induced by MDCK-SH cells and Pri-SH cells. In addition, Pri-SH cells also carried original stable cell line properties, with decreased E-cadherin levels and increased Vimentin and N-cadherin levels.

3.4. E-cadherin and NMMIIA are Kif5b cargoes and their levels are decreased in Kif5b depleted epithelial cells

Knockdown of Kif5b in MDCK cells caused a significant defect in expression level of E-cadherin, suggesting that Kif5b is possibly involved in the transport of E-cadherin. To further verify the possible interaction between Kif5b and E-cadherin, and to identify other cargo candidates, Co-IP was used to investigate Kif5b interacting proteins in polarized MDCK cells (three days after confluence). Fig. 3G shows a representative SDS-PAGE gel for Co-IP products stained by silver nitrate. A protein with molecular weight larger than 170 kD was found to be co-immunoprecipitated with Kif5b. This protein was identified as myosin heavy peptide 9 (MYH 9) (non-muscular myosin IIA (NMMIIA)) (Supplementary Table 1). The interaction between Kif5b and E-cadherin, NMMIIA was confirmed by Western blot of Co-IP products (Fig. 3H). Furthermore, Western blot revealed that both E-cadherin and NMMIIA expression levels were decreased in Kif5b-deficient cells compared with control cells (Fig. 3F). Similar results were observed in Kif5b deleted mouse kidneys (Supplementary Fig. 2b). However overexpression of E-cadherin and NMMIIA in the original stable cells could reverse the expression patterns of N-cadherin and vimentin (Fig. 4A), as well as the cell migration ability (Fig. 4B), suggesting that EMT in Kif5b deficient MDCK cells was result from down-regulation of E-cadherin and NMMIIA.

4. Discussion

In this study, it was found that Kif5b deficient MDCK cells had a decreased cell proliferation rate, which is concomitant with a higher proportion of cells in the G_0-G_1 phase and a lower proportion of cells in the G_2/M phases. An increased proportion of cells in G_0-G_1 phase indicate that biosynthesis for DNA duplication was delayed in Kif5b-depleted MDCK cells. Meanwhile, more binucleated cells are present after depletion of Kif5b in MDCK cells, indicating a requirement of Kif5b for mitosis or cytokinesis. Possible roles of Kif5b in spindle formation, chromosome congression and alignment, as well as cytokinesis are unknown, and need to be further investigated.

To reveal the underlying mechanisms for epithelial–mesenchymal transition resulted from knockdown of Kif5b, Co-IP was used to identify Kif5b cargo candidates. E-cadherin and NMMIIA have been revealed to be Kif5b partners in MDCK cells. Moreover, protein levels of E-cadherin and NMMIIA are decreased after knockdown of Kif5b.

E-cadherin is a Ca^{2+}-dependent transmembrane protein that can form adherens junctions in polarized epithelial cells. Intracellular domains of E-cadherin can bind with β-catenin-α-catenin complex and be further linked to the F-actin belt [14]. E-cadherin null mice die at an early embryonic stage and fail to form trophectodermal epithelium, indicating that E-cadherin is essential for epithelium biogenesis [15]. Conditional knockout of

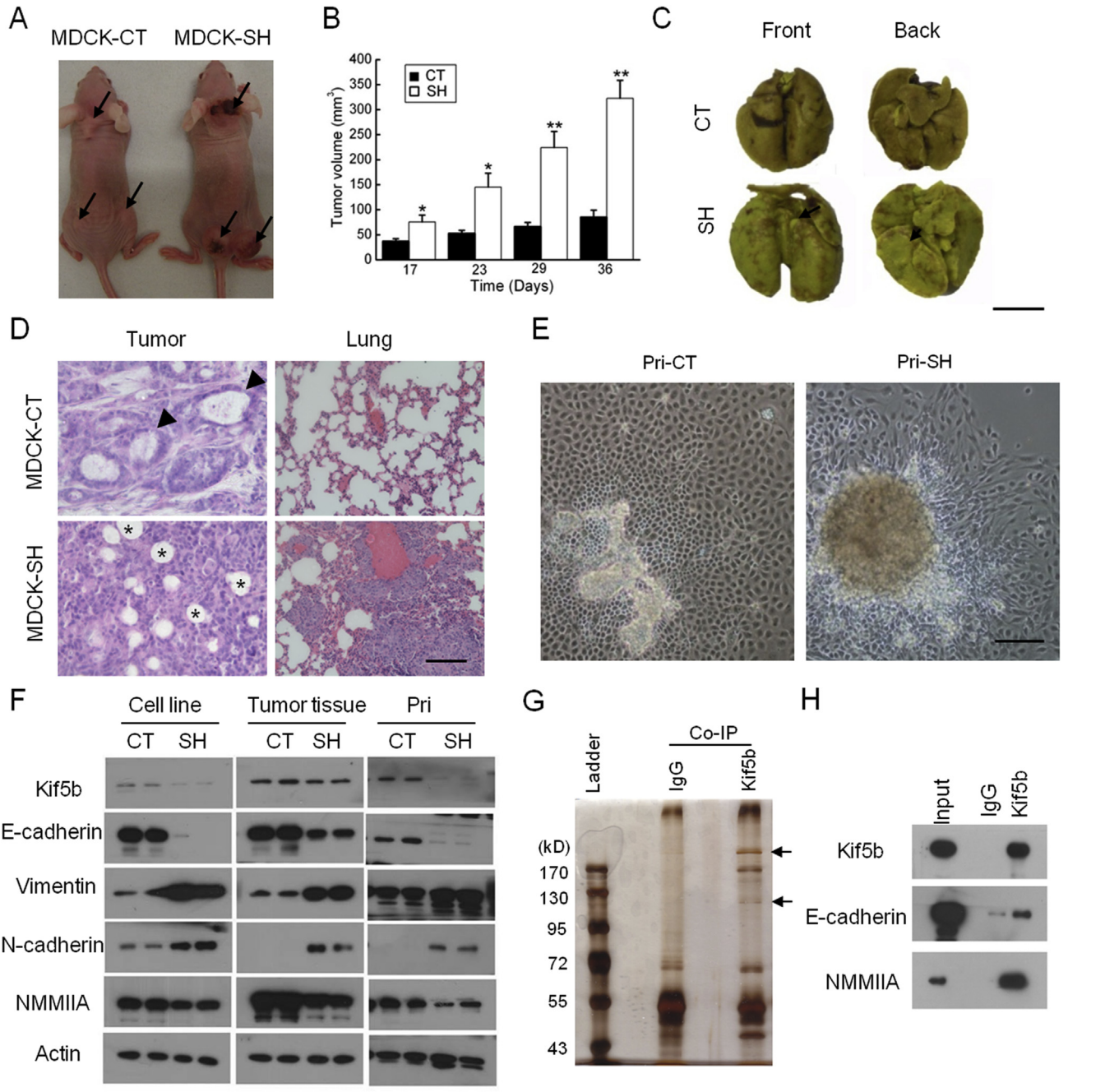

Fig. 3. Remarkable increase in tumorigenesis and visible metastatic foci on lungs of mice injected by MDCK-SH cells. (A) A representative photograph of nude mice bearing tumors. Identical results were obtained in five mice received five independently isolated transfectant clones. (B) Statistical analysis of tumor volumes at indicated time points. Tumor volume is calculated according to the fomular: $V = 4/3 \times \pi \times L \times D^2/8$, where L = length, D = width, *P < 0.05, **P < 0.01, n = 5 mice. (C) Lungs were fixed and stained with Bouin's solution. Many metastatic foci were visible in the lungs of mice injected with MDCK-SH cells. Scale bar = 5 mm. (D) Histological examination of tumor tissues and lungs. Arrow heads, tubules; asterisks, vacuoles. Scale bar = 50 μm. (E) Primary culture of tumor tissues. Scale bar = 50 μm. (F) Western blot analysis of protein expression levels. CT, control; SH, Kif5b knockdown. Actin was used as an internal control. Samples were loaded in duplication. (G) Silver staining of Co-IP products from polarized MDCK cells. Normal rabbit IgG was used as a negative control. (H) E-cadherin and NMMIIA could be co-immunoprecipitated with Kif5b in polarized MDCK cells.

E-cadherin in stratified epithelium of skin leads to mislocalization of tight junction markers, resulting in failure to retain water [16]. These *in vivo* studies demonstrate that E-cadherin is essential for epithelial polarity formation. Nonmuscle myosin II (NMMII) is also associated with the F-actin belt at the basolateral domains of epithelial cells [17]. Inhibition of NMMII by blebbistatin can block F-actin reorganization and disassembly of junction complexes, indicating a requirement of NMMII for actin filament contraction and adherens junction disassembly [18]. Interactions between KHC and p120 [8], dynein and β-catenin [19] suggest that microtubules also participate in regulation of adherens junctions. A later study using a Ca^{2+} switch model demonstrates that microtubules can regulate F-actin reorganization and junctional disassembly, which is mediated by Kinesin-1 [9]. All these studies indicate crosstalk between microtubules and actin filaments as well as their associated motors. Co-sedimentation of microtubules and NMMII in the rat brain [20], as well as interactions between Kif5b and nonmuscular

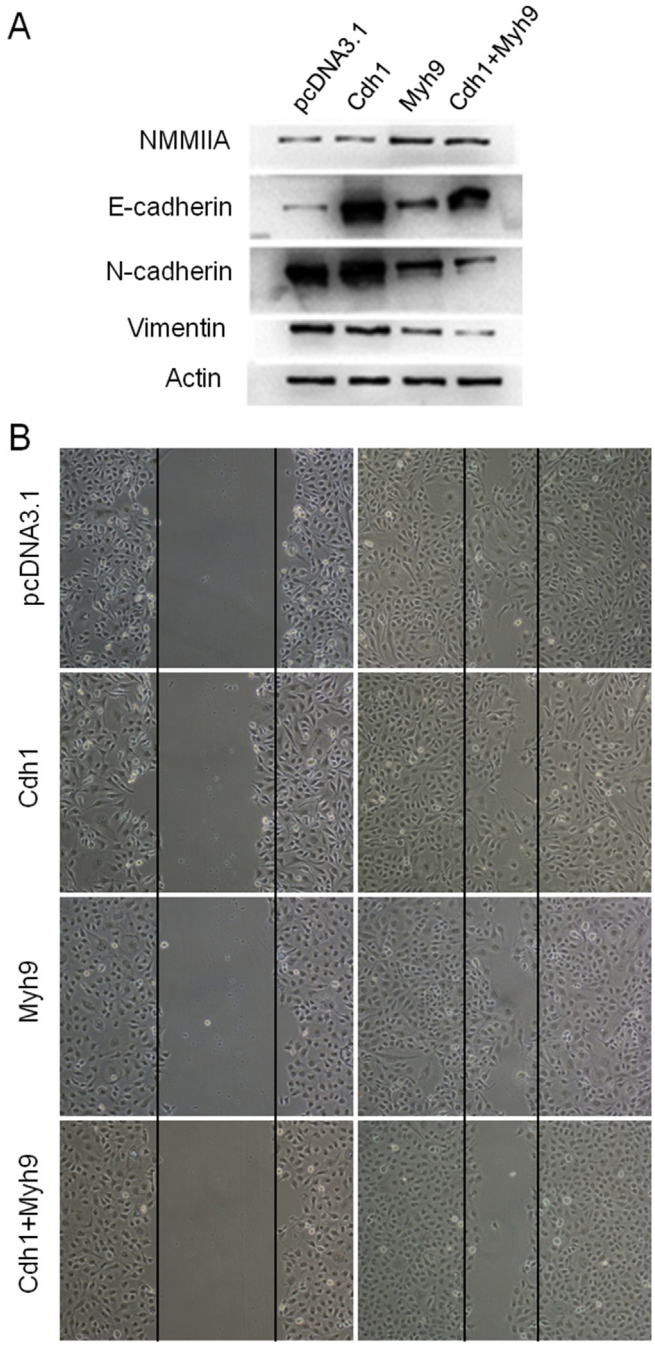

Fig. 4. Overexpression of E-cadherin and NMMIIA in the original stable cells reverses the EMT phenotypes of Kif5b deficient MDCK cells. (A) overexpression of E-cadherin and NMMIIA leads to the down regulation of N-cadherin and vimentin. (B) The mobility behavior of cells was analyzed in an *in vitro* wound-healing model. Cells were transfected with indicated plasmids 24 h before the incision was made and photographs were taken immediately after incision (left panel) and after 24 h in culture (right panel).

myosin IIA (NMMIIA) revealed by this study, do confirm the links between microtubules and actin filaments, which is mediated by interactions of their motor proteins.

NMMII is a motor protein composed of two heavy chains and two light chains [21]. Three isoforms for NMMII heavy chains have been identified in mammalian cells, including NMMIIA, NMMIIB, and NMMIIC [22]. Although all isoforms are located at the F-actin belt, only NMMIIA has been demonstrated to regulate epithelial apical junctions [17]. Knockdown of NMMIIA in human intestinal epithelial cells (SK–CO15) results in significant morphological and physiological changes, which is characterized by a fibroblast-like shape, a profound reduction in transepithelial electrical resistance [17],

Based on these pioneering findings, it can be suspected that down-regulation of E-cadherin and NMMIIA in Kif5b-deficient MDCK cells contributes to the epithelial–mesenchymal transition observed in this study. Interactions between Kif5b and E-cadherin, NMMIIA revealed by Co-IP suggest a native link among microtubule, F-actin belt, and cell junction complexes. Kif5b may work upstream in this biological chain. In unpolarized epithelial cells, microtubules are nucleated near the Golgi network with the plus end pointing to the cell periphery. E-cadherin and NMMIIA are transported by Kif5b from the trans-Golgi to specific destinations along microtubules. At the cell membrane, active plus ends of microtubules regulate focal accumulation of E-cadherin [23]. The extracellular domain of concentrated E-cadherin can mediate contacts between neighboring cells to initiate adherens junction and tight junction formation. Meanwhile, NMMIIA moves on actin filaments at the cell periphery to facilitate F-actin belt formation, which can reinforce the maturation of cell junctions. Developed cell junctions coordinate the polarized distribution of plasma membrane proteins and cell cytoskeleton reorganization, including F-actin belt formation and apicobasolateral alignment of microtubules, to realize polarity formation. Knockdown of Kif5b attenuates intracellular transport of E-cadherin and NMMIIA, and down-regulates the cellular levels of these proteins through some unidentified pathways. Insufficient levels of NMMIIA, E-cadherin and Kif5b result in cell morphological changes, failure of polarity formation, and reprogramming of gene expression. As a result, MDCK cells cannot sustain epithelial propertied or go through epithelial–mesenchymal transition.

In conclusion, this study suggests that Kif5b mediated intracellular transportation plays an important role during epithelial cell polarity formation, probably by participating in regulation of cell–cell contacts.

Conflict of interest

The authors declare that there is no conflict of interest.

Acknowledgments

This work was supported by grants from the Hong Kong Research Grants Council (HKU 768113M, HKU 767012) to JDH, a grant from the National Natural Science Foundation of China (31400995) and a grant from the Beijing Municipal Natural Science Foundation (7154234) to JC.

Appendix A. Supplementary data

Supplementary data related to this article can be found at http://dx.doi.org/10.1016/j.bbrc.2015.05.045.

Transparency document

Transparency document related to this article can be found online at http://dx.doi.org/10.1016/j.bbrc.2015.05.045.

References

[1] M.R. Wallenfang, G. Seydoux, Polarization of the anterior-posterior axis of *C. elegans* is a microtubule-directed process, Nature 408 (2000) 89–92.
[2] B. Albert, A. Johnson, J. Lewis, Molecular Biology of the Cell, 4 ed., Garland Science, New York, 2002.

[3] F. Lafont, J.K. Burkhardt, K. Simons, Involvement of microtubule motors in basolateral and apical transport in kidney cells, Nature 372 (1994) 801–803.
[4] S. Fan, T.W. Hurd, C.J. Liu, S.W. Straight, T. Weimbs, E.A. Hurd, S.E. Domino, B. Margolis, Polarity proteins control ciliogenesis via kinesin motor interactions, Curr. Biol. 14 (2004) 1451–1461.
[5] Y. Noda, Y. Okada, N. Saito, M. Setou, Y. Xu, Z. Zhang, N. Hirokawa, KIFC3, a microtubule minus end-directed motor for the apical transport of annexin XIIIb-associated triton-insoluble membranes, J. Cell. Biol. 155 (2001) 77–88.
[6] F. Jaulin, X. Xue, E. Rodriguez-Boulan, G. Kreitzer, Polarization-dependent selective transport to the apical membrane by KIF5B in MDCK cells, Dev. Cell. 13 (2007) 511–522.
[7] H.E. Trejo, E. Lecuona, D. Grillo, I. Szleifer, O.E. Nekrasova, V.I. Gelfand, J.I. Sznajder, Role of kinesin light chain-2 of kinesin-1 in the traffic of Na,K-ATPase-containing vesicles in alveolar epithelial cells, FASEB J. Off. Publ. Fed. Am. Soc. Exp. Biol. 24 (2010) 374–382.
[8] X. Chen, S. Kojima, G.G. Borisy, K.J. Green, p120 catenin associates with kinesin and facilitates the transport of cadherin-catenin complexes to intercellular junctions, J. Cell. Biol. 163 (2003) 547–557.
[9] A.I. Ivanov, I.C. McCall, B. Babbin, S.N. Samarin, A. Nusrat, C.A. Parkos, Microtubules regulate disassembly of epithelial apical junctions, BMC Cell. Biol. 7 (2006) 12.
[10] J. Cui, X. Li, Z. Duan, W. Xue, Z. Wang, S. Lu, R. Lin, M. Liu, G. Zhu, J.D. Huang, Analysis of Kif5b expression during mouse kidney development, PloS One 10 (2015) e0126002.
[11] J. Cui, Z. Wang, Q. Cheng, R. Lin, X.M. Zhang, P.S. Leung, N.G. Copeland, N.A. Jenkins, K.M. Yao, J.D. Huang, Targeted inactivation of kinesin-1 in pancreatic beta-cells in vivo leads to insulin secretory deficiency, Diabetes 60 (2011) 320–330.
[12] E.D. Hay, An overview of epithelio-mesenchymal transformation, Acta Anat. (Basel) 154 (1995) 8–20.
[13] J.P. Thiery, H. Acloque, R.Y. Huang, M.A. Nieto, Epithelial-mesenchymal transitions in development and disease, Cell 139 (2009) 871–890.
[14] W. Meng, M. Takeichi, Adherens junction: molecular architecture and regulation, Cold Spring Harb. Perspect. Biol. 1 (2009) a002899.
[15] L. Larue, M. Ohsugi, J. Hirchenhain, R. Kemler, E-cadherin null mutant embryos fail to form a trophectoderm epithelium, Proc. Natl. Acad. Sci. U S A. 91 (1994) 8263–8267.
[16] J.A. Tunggal, I. Helfrich, A. Schmitz, H. Schwarz, D. Gunzel, M. Fromm, R. Kemler, T. Krieg, C.M. Niessen, E-cadherin is essential for in vivo epidermal barrier function by regulating tight junctions, Embo J. 24 (2005) 1146–1156.
[17] A.I. Ivanov, M. Bachar, B.A. Babbin, R.S. Adelstein, A. Nusrat, C.A. Parkos, A unique role for nonmuscle myosin heavy chain IIA in regulation of epithelial apical junctions, PLoS One 2 (2007) e658.
[18] A.I. Ivanov, I.C. McCall, C.A. Parkos, A. Nusrat, Role for actin filament turnover and a myosin II motor in cytoskeleton-driven disassembly of the epithelial apical junctional complex, Mol. Biol. Cell. 15 (2004) 2639–2651.
[19] L.A. Ligon, S. Karki, M. Tokito, E.L. Holzbaur, Dynein binds to beta-catenin and may tether microtubules at adherens junctions, Nat. Cell. Biol. 3 (2001) 913–917.
[20] T. Sakamoto, A. Uezu, S. Kawauchi, T. Kuramoto, K. Makino, K. Umeda, N. Araki, H. Baba, H. Nakanishi, Mass spectrometric analysis of microtubule co-sedimented proteins from rat brain, Genes. Cells 13 (2008) 295–312.
[21] E.M. De La Cruz, E.M. Ostap, Relating biochemistry and function in the myosin superfamily, Curr. Opin. Cell. Biol. 16 (2004) 61–67.
[22] E. Golomb, X. Ma, S.S. Jana, Y.A. Preston, S. Kawamoto, N.G. Shoham, E. Goldin, M.A. Conti, J.R. Sellers, R.S. Adelstein, Identification and characterization of nonmuscle myosin II-C, a new member of the myosin II family, J. Biol. Chem. 279 (2004) 2800–2808.
[23] S.J. Stehbens, A.D. Paterson, M.S. Crampton, A.M. Shewan, C. Ferguson, A. Akhmanova, R.G. Parton, A.S. Yap, Dynamic microtubules regulate the local concentration of E-cadherin at cell-cell contacts, J. Cell. Sci. 119 (2006) 1801–1811.